Fibroblast Growth Factor 21 Ameliorates Hyperuricemic Nephropathy By Improving Oxidative Stress Through Activating Akt/Nrf2 Signaling Pathway

Xinghao Jiang
Northeast Agricultural University
Yimeng Zou
Northeast Agricultural University
Yeboah Kwaku opoku
Department of Biology Education, Faculty of Science Education , University of Education
Shijie Liu
Northeast Agricultural University
Dan Wang
Northeast Agricultural University
Kai Kang
Northeast Agricultural University
Deshan Li
Northeast Agricultural University
Guiping Ren (renguiping@126.com)
Northeast Agricultural University https://orcid.org/0000-0001-8202-5380

Research Article

Keywords: FGF21, Hyperuricemic nephropathy, Oxidative stress, Akt/Nrf2 pathway

Posted Date: June 25th, 2021

DOI: https://doi.org/10.21203/rs.3.rs-405082/v2

Abstract

Epidemiological investigations have shown an elevated expression of circulating fibroblast growth factor 21 (FGF21) of patients with hyperuricemia. However, the effect of FGF21 on hyperuricemic nephropathy (HN) is still unknown. The purpose of this study, therefore, was to explore the effect and mechanism of action of FGF21 on HN. The level of FGF21 in peripheral blood mononuclear cells (PBMCs) was determined in 10 patients with HN. *In vivo* models of HN were induced in C57BL/6 mice. Six mice in each group were treated with FGF21 at a dose of 1mg/kg and 5mg/kg for 30 days. For the *in vitro* studies, glomerular mesangial cells (GMCs) were exposed to lipopolysaccharide and monosodium uric acid to induce inflammation and oxidative stress. This was followed by treatment with 100nM, 1000nM of FGF21 for 72 h to observe the therapeutic effect. The levels of FGF21 in patients with HN were elevated. Also, we found that exogenous injection of FGF21 could significantly improve kidney injury in HN mice. This was characterized by a decrease in inflammatory factors and fibrosis and the improvement of oxidative stress. FGF21 recorded a significant therapeutic effect through the activation of Nrf2 in both *in vivo* and *in vitro* studies. However, the effect of enhancement of FGF21 on Nrf2 was reduced by the addition of Akt inhibitor GSK690693. In conclusion, our study found for the first time that FGF21 can significantly improve HN through the promotion of the Akt/Nrf2 signalling pathway leading to improvement in oxidative stress.

Introduction

Hyperuricemic nephropathy (HN) is a kidney disease characterized by primary or secondary hyperuricemia accompanied by interstitial inflammation, fibrosis, renal calculi, and acute or chronic renal failure caused by uric acid (or urate) deposition in the kidney [1]. Uric acid is the final product of purine metabolism, and about 70% of it is excreted through the kidney [2]. When the concentration of uric acid exceeds the normal physiological range, it leads to various pathological reactions. Xanthine oxidoreductase (XOR) is an important enzyme involved in the degradation of purine nucleotides. It oxidizes hypoxanthine to xanthine, which in turn catalyzes the oxidation of xanthine to uric acid. In this process, reactive oxygen species (ROS) are produced as by-products with their accumulation leading to oxidative stress [3]. Studies have shown that oxidative stress can activate inflammation and fibrotic pathways leading to kidney damage [3–5]. Therefore, the inhibition of oxidative stress may significantly improve renal injury in hyperuricemia. Studies have also shown a yearly increase in the global incidence of hyperuricemia and it has become a metabolic disease second to diabetes and hyperlipidemia [6]. Selective XO inhibitors, febuxostat, and allopurinol are currently used in the clinical management of hyperuricemia and its related complications [7]. However, the long-term use of these drugs in some people leads to allergic reactions, progressive decline of red blood cells, diarrhoea, vomiting, and other adverse reactions accompanied by serious nephrotoxicity. These observations lead to apathy for these drugs in patients with HN [8, 9]. Besides, some meta-analyses concluded that currently there is insufficient evidence to support the use of urate lowering therapy (ULT) for treatment of HN progression [10]. Therefore, it is necessary for the search for novel therapeutics for the management and treatment of HN.

Fibroblast growth factor (FGF) 21 was first isolated from mouse embryos by Nishimura et al [11]. It has a signal protein with a conserved core domain (about 120 amino acids). These molecules have many functions, including embryo development, tissue regeneration, and maintenance of metabolic homeostasis [12]. FGF21 is mainly expressed in liver tissues but can also be detected in kidney tissues, lymphatic tissues, fat tissues and skeletal muscle [13, 11, 14]. FGF21 is a special member of the FGF family and forms a subfamily with FGF19 and FGF23. Although most other FGFs interact with cell surface-related heparan sulfate (HS) proteoglycan, these three unique FGFs show great reduction or no HS binding, which enables them to leave their tissue of origin to function in an endocrine manner [15]. FGF21 initially attracted the interest of the scientific community due to its ability to improve glucose and lipid metabolism. Studies have shown that exogenous FGF21 can significantly reduce blood sugar in diabetic rats, dogs and monkeys [16–18]. In addition, the weight of obese model mice decreased significantly after FGF21 treatment [19]. In recent years, it has been found that FGF21 has significant anti-inflammatory effects leading to the inhibition of rheumatoid arthritis and inflammatory response in the pancreas induced by a high-fat diet and glucose [16, 19, 20]. Hence, FGF21 may be a beneficial factor in metabolic diseases. Hyperuricemia has been shown to be one of the main risk factors associated with these metabolic diseases [21]. However, the effect of FGF21 on HN has not been reported. Therefore, the purpose of this study is to determine the effect of FGF21 on the progression of nephropathy in hyperuricemia and to further explore the associated molecular mechanisms to provide new ideas for the treatment of HN.

Materials And Methods

Patients

All study participants signed written consent forms to be enrolled in the study with the confidentiality of their data assured. This study was approved by the Ethics Committee of the Endocrinology Department of Harbin First Hospital. Serum samples (20) were obtained from Harbin First Hospital, including 10 patients with hyperuricemic nephritis and 10 healthy individuals. The details of the patients with HN are as follows: patients 1 to 9, males, aged 28, 35, 35, 40, 45, 52, 55, 57, 59 with hyperuricemic interstitial glomerulonephritis, six of them were on allopurinol while three of them took febuxostat before the blood sample was taken. Patient 10, male, 65 years old, suffering from diabetes, hyperuricemia, and chronic renal failure who has been on febuxostat and insulin for a long time. The 10 healthy people were males, aged between 26 and 57 years old. Human peripheral blood mononuclear cells (PBMCs) were extracted with a PBMCs separation kit (Haoyang Biological products Technology Co., Ltd., Tianjin) followed by the Trizol method for the extraction of RNA or real-time quantitative PCR (qPCR) detection.

Animals

Male wild-type (WT) C57BL/6 mice, 8 weeks old, were purchased from Liaoning Changsheng Biological Co., Ltd. All mice were kept in cages fitted with air supply filters at 22 ~ 26℃, with a relative humidity of 40%~45% and a light-dark period of 12 hours, and were fed ad libitum. All animal studies were conducted

in accordance with the guidelines formulated by the Animal Protection and Utilization Committee of Northeast Agricultural University.

Acquisition of FGF21

Human FGF21 was selected for this study. Recombinant SUMO-FGF21 plasmid was added to the *E. coli* competent cell Rossetta (Bioengineering technology company, Shanghai) followed by bacteria fermentation. After the fermentation process, the cells were collected, the supernatant was extracted, and the SUMO-FGF21 protein was obtained by His Trap TM FF crude Colum (GE Health, USA) affinity chromatography. The SUMO-FGF21 complex was digested with SUMO protease for 8 hours followed by a second affinity chromatography to finally obtain the mature FGF21 protein. The molecular weight and purity of the FGF21 protein were analyzed by SDS polyacrylamide gel electrophoresis (SDS-PAGE) and high-performance liquid chromatography (HPLC).

Grouping and establishment of HN model in mice

Mice models of HN were given adenine (160mg/kg) and potassium oxysalt (2400mg/kg) (Sigma-Aldrich, USA) [22] by gavage while the normal controls were given intragastric administration of saline at the same volume once a day for 30 days. The experimental animals were grouped into 4 as follows: normal control group, model control group, FGF21 low dose group, and FGF21 high dose group. The specific treatment regimens were as follows: low dose FGF21 (1mg/kg) group, (n = 6): FGF21 was injected intraperitoneally every day for 30 days; high dose FGF21 (5mg/kg) group, (n = 6): FGF21 was injected intraperitoneally every day for 30 days; normal control (n = 6) and model control group (n = 6): intraperitoneal injection of the same volume of normal saline every day for 30 days. Two doses of FGF21 were decided according to the previous study in mice with pulmonary fibrosis [23]. At the end of the study, the mice were euthanized and blood and kidney samples were taken for further analysis.

Detection of renal function

Serum samples from the collected blood samples were isolated and sent to the Harbin Electric Power Hospital for the detection of renal function indices such as blood urea nitrogen (BUN), Serum creatinine (Scr), cystatin C (CysC), and β 2-microglobulin (β2-MG).

Histopathological examination

Sample kidney tissues from the different experimental groups were fixed in 4% paraformaldehyde for 7 days, then dehydrated and embedded in paraffin. Tissue sections (7μm) were cut using a microtome (Lecia, Germany), and then fully stretched in a water bath at 42℃. The sections were then transferred to a glass slide for hematoxylin-eosin (H&E) staining or Masson staining. Finally, the blue area stained by Masson staining was observed under an inverted optical microscope and was analyzed by Image J software.

Immunohistochemistry

The prepared paraffin sections were put into an oven at 60℃ for one hour and then dewaxed in xylene and ethanol with different concentration gradients. After dewaxing, the antigen was repaired followed by incubation with anti F4/80 antibody (dilution: 1:200, Abcam, USA) at 4 ℃ for 12 hours. The slides were washed twice with PBS followed by incubation with goat anti-rabbit secondary antibody (R&D, USA) at 37 ℃ for 1 hour. Again, the slides were washed twice with PBS and the reaction visualized with diaminobenzidine (DAB) for 8 minutes. The reaction was terminated by rinsing with water followed by hematoxylin-eosin staining. Finally, the slide sections were observed under an inverted optical microscope and the results analyzed by Image J software.

Cell culture

Mouse Glomerular Mesangial cells (GMCs) (ATCC, USA) were cultured in Dulbecco's modified eagle's medium (DMEM) (70%) and Ham's F12 nutrient medium (25%) containing 5% fetal bovine serum (FBS) (Gibco, NY, USA). The concentration of penicillin and streptomycin in the culture medium was 100U/ml and cultured in a 37 ℃ incubator with 5% carbon dioxide. After fusion of the GMCs cells for about 80%, the culture medium was discarded, washed with PBS for 3 times, and a serum-free medium was added to the 24-well plate. The cells were given lipopolysaccharide (LPS) at a concentration of 500ng/ml followed by monosodium uric acid (MSU) (Sigma, USA) at a concentration of 0, 100, 200, 400, 800, and 1600ng/ml (2 wells per concentration). The cells were then stimulated for a period of 24 hours. Finally, protein expression of IL-1β was estimated to determine the best concentration and period of action of MSU. After determining the optimal concentration and action time of MSU, 100nM and 1000nM of FGF21 were added to the cells to observe the therapeutic effect. These two doses were determined based on previous studies [24]. For the study of inhibition of Protein kinase B (Akt), GMCs cells were grown in a medium containing 10μM GSK690693 (an Akt inhibitor) (Beyotime, Shanghai). At the end of the study, the cells were collected for qPCR, Elisa and Western blotting analysis.

qPCR

Total RNA was extracted from the kidney of the mice using Trizol reagent (Takara Company, Japan). cDNA was synthesized by reverse transcription and the expression of the target genes were analyzed by qPCR using Quanti Tet SYBR Green PCR kit (Takara Company, Japan). The relative content of the target genes was calculated relative to that of the normal group. The primers used in this study were as follows: GAPDH (human) forward: ACAACTTTGGTATCGTGGAAGG reverse: GCCATCACGCCACAGTTTC; β-actin (mouse) forward: GGCTGTATTCCCCTCCATCG reverse: CCAGTTGGTAACAATGCCATGT; FGF21 (human) forward: TTTACCAGTCCGAAGCCCAC reverse: CCTGGTAGTGGCAGGAAGC; FGF21 (mouse) forward: CTGCTGGGGGTCTACCAAG reverse: CTGCGCCTACCACTGTTCC; NACHT, LRR and PYD domains-containing protein 3 (NLRP3) (mouse) forward: CTCCAACCATTCTCTGACCAG reverse: ACAGATTGAAGTAAGGCCGG; Collagen 1 (Col 1) (mouse) forward: GTGCTAAAGGTGCCAATGGT reverse: ACCAGGTTCACCGCTGTTAC; α-smooth muscle actin (α-SMA) (mouse) forward: CGGGACATCAAGGAGAAACT reverse: CCCATCAGGCAACTCGTAA; interleukin (IL)-1β (mouse) forward: TCGCCAGTGAAATGATGGCTTA reverse: GTCCATGGCCACAACAACTGA; tumor necrosis factor (TNF)-α (mouse) forward: ATGAGCACTGAAAGCATGATC reverse: TCACAGGGCAATGATCCCAAAGTAGACCTGCCC;

IL-6 (mouse) forward: ACTCACCTCTTCAGAACGAATTG reverse: CCATCTTTGGAAGGTTCAGGTTG; IL-10 (mouse) forward: TGGACAACATACTGCTAACCGAC reverse: TGGACAACATACTGCTAACCGAC.

Elisa analysis

The FGF21 content in human serum was detected by human FGF21 Elisa kit (Andy Gene Biotechnology Co., LTD, Beijing, China). Radioimmunoprecipitation assay (RIPA) solution and protease inhibitor (Beyotime Biotechnology, Shanghai, China) were added to the preserved kidney tissues, ground, and crushed using medical tissue homogenizer to finally extracted the supernatant. The expressions of FGF21, IL-1β, TNF- α, IL-6, IL-10, reactive oxygen species (ROS), malondialdehyde (MDA), catalase (CAT), superoxide dismutase (SOD), glutathione reductase (GR), glutathione peroxidase (GSH-PX), and hydroxyproline were detected by mouse Elisa kit (Andy Gene Biotechnology Co., LTD, Beijing, China) after protein extraction from the kidney of the mice and GMCs. Nuclear proteins of tissues or cells are extracted by Nuclear Protein Extraction Kit (Beyotime Biotechnology, Shanghai, China).

Western blotting

The concentrations of the proteins extracted from the kidney tissues and GMCs were determined by BCA kit (Beyotime, Shanghai). Equal amounts of protein samples were separated by SDS-PAGE and then transferred to a nitrocellulose membrane. After sealing for 10 minutes at room temperature with rapid sealing solution, primary antibodies anti-NLRP3 (dilution: 1: 1000, Abcam, USA), anti-Col1 (dilution: 1: 1000, Abcam, USA), anti-α-SMA (dilution: 1: 1000, Abcam, USA), anti-nuclear factor E2-related factor 2 (Nrf2) (dilution: 1: 1000, Abcam, USA), anti-AKT (dilution: 1: 1000, Abcam, USA) and anti-p (Thr 308) AKT (dilution: 1: 1000, Abcam, USA) were added at 4℃ for 12h. This was followed by incubation with a secondary antibody, horseradish peroxidase-coupled (HRP) (dilution: 1: 3000, R&D, USA) at 37℃ for 1 h. Blots were developed with an Electro-Chemi-Luminescence (ECL) kit (Amersham Biosciences, Piscataway, NJ), and the results quantified using ImageJ software.

Statistical analysis

Data were analyzed with GraphPad Prism 7.0 software for windows. Mean ± SD values were calculated, and one-way ANOVA was used to test for significance at $P < 0.05$. Tukey's Post hoc analysis was further used for comparison between groups.

Results

Increased expression of FGF21 in both humans and mice with HN

The expression level of the FGF21 gene and protein was analyzed by qPCR and Elisa. The results showed that the average mRNA content of FGF21 in PBMCs of patients with HN was 0.83 times higher than that of healthy people and the average protein content of FGF21 in serum of patients with HN was 1.88 times higher than that of healthy people, and the difference was significant ($P < 0.05$) (Fig. 1a, b). In addition,

the average content of FGF21 mRNA and protein in the kidney of HN mice was 0.45 times and 0.55 times higher than that of the normal group, and the difference was statistically significant ($P < 0.05$) (Fig. 1c, d). Again, the above results indicate that the levels of FGF21 increase in HN. However, whether FGF21 inhibits or promotes HN needs to be further investigated.

FGF21 ameliorates renal function damage in HN mice

At the end of the animal experiment, serum samples of the mice were separated from whole blood samples for the detection of indices of renal function. The results showed that the renal function of mice in the model group was severely impaired characterized by a significant increase in BUN, Scr, CysC, and β2-MG ($P < 0.01$). However, treatment with different doses of FGF21 was marked by a significant improvement in renal function indices in HN mice ($P < 0.01$) with the high dose recording a better therapeutic effect (Fig. 2a-d). H&E staining also revealed significant damage to the kidneys of the model mice. The damage was characterized by inflammatory cell infiltration between renal tissues, vacuolar degeneration, tubular atrophy, and glomerular hyperemia. These pathological injuries were, however, significantly improved after treatment with FGF21 (Fig. 2e).

FGF21 reduced renal inflammation in HN mice

Immune system activation and subsequent infiltration of macrophages play an important role in the occurrence and development of renal injury [25]. Therefore, we observed the infiltration of macrophages in the kidney of HN mice by immunohistochemistry using F4/80 antibody. Increased macrophage infiltration in the kidney of the model was recorded, an indication of severe inflammatory. This was however abated significantly after treatment with FGF21 ($P < 0.01$) (Fig. 3a, b). Again, FGF21 significantly reduced inflammatory factors such as IL-1β, TNF- α, and IL-6 tied to increasing the levels of IL-10 compared with the model group ($P < 0.05$) (Fig. 3c, d). Interestingly, the level of anti-inflammatory factor IL-10 in the model group was also significantly higher than that in the normal group, which may be a manifestation of the body's response to inflammation ($P < 0.01$) (Fig. 3c, d). Also, the levels of NLRP3, a marker of inflammation, were significantly increased in kidney tissues at both gene and protein levels in the model group compared to the normal group ($P < 0.01$). Once again, a significant reduction of NLRP3 marked treatment with the low and high doses of FGF21 ($P < 0.05$) (Fig. 3e-g). These results intimate the anti-inflammatory effect of FGF21 in renal injury associated with hyperuricemia.

FGF21 improves renal fibrosis in HN mice

In order to observe the degree of fibrosis in the kidney of the mice, Masson staining was used to determine the collagen content within the kidney. Compared with the normal group, the positive areas in the kidney of the model group were significantly increased ($P < 0.01$). This was, however, reduced significantly in the FGF21 treatment group ($P < 0.01$) (Fig. 4a, b). Also, the hydroxyproline content in the kidney of the FGF21 treatment group was significantly lowered compared to the model group ($P < 0.01$) (Fig. 4c). In addition, markers of fibrosis such as Col1, α-SMA, and TGF-β were also detected. The mRNA and protein levels of Col1, α-SMA, and TGF-β in the model group were significantly higher compared with the normal group ($P < 0.01$). FGF21 treatment, however, was marked by a significant reduction in Col1, α-

SMA, and TGF-β levels in the kidney both at the mRNA and protein levels ($P < 0.05$) (Fig. 4d-f). These results suggest that FGF21 can inhibit the development of renal fibrosis in HN mice.

FGF21 ameliorates oxidative stress in HN mice

After the observation that FGF21 could significantly improve HN, the possible contributing mechanisms were explored. Oxidative stress can promote inflammation and fibrosis [5], therefore, oxidative stress indices were detected. Compared with the normal group, the amount of ROS and MDA in the model group increased significantly ($P < 0.01$) (Fig. 5a, b). However, FGF21 treatment significantly inhibited the levels of ROS, MDA and increased the levels of antioxidant enzymes CAT, SOD, GR, and GSH-PX (Fig. 5c-f) ($P < 0.01$). The activation of the Nrf2 signal pathway plays an important role in the antioxidant process as it triggers the production of various antioxidant response elements (AREs) [26]. Western blotting results showed that compared with the model group, both the low and high doses of FGF21 significantly increased the nuclear accumulation of Nrf2 ($P < 0.05$). In addition, the level of pAkt/Akt was also significantly improved compared with the model group ($P < 0.01$) (Fig. 5g, h). However, whether FGF21 activates Nrf2 through Akt needs further proof.

FGF21 ameliorates oxidative stress through Akt/Nrf2 signal pathway in GMCs cells

Elisa results showed a gradual increase in the concentration of MSU and action time with the expression of IL-1β with a peak concentration of MSU at 800ng/ml and an action time of 72h (Fig. 6a, b). These conditions were therefore used for the experimental model cells. We then detected the expression of inflammatory factors in the cells. Compared with the model group, the FL and FH groups significantly inhibited the expression of inflammatory factors such as IL-1β, TNF-α, IL-6 ($P < 0.05$) and increase the expression level of anti-inflammatory factor IL-10 ($P < 0.05$) (Fig. 6c, d). Additionally, the relationship between FGF21 and oxidative stress in the GMCs was observed. Elisa results showed that compared with the model group, the FL and FH groups significantly inhibited the expression of ROS and MDA ($P < 0.01$), and increased the levels of expression of antioxidant enzymes CAT, SOD, GR, and GSH ($P < 0.05$) (Fig. 6e). The expressions of Nrf2, Akt, and pAkt in GMCs were also detected. The results showed that the Nrf2 and pAkt/Akt levels in the FL and FH groups were significantly higher compared to the model group ($P < 0.05$) (Fig. 6f-i). However, when GSK690693 was used to inhibit the expression of Akt, there was no significant difference in the expression of Nrf2 between the FL, FH, and the model group. This is, however, indicative of the fact that FGF21 activates Nrf2 through Akt (Fig. 6h, i).

Discussion

In recent years, the incidence of HN is gradually increasing [6]. Traditional therapeutic drugs such as benzbromarone, allopurinol, and febuxostat are accompanied by severe hepatorenal toxicity, which is not suitable for all patients [8, 9]. Therefore, the development of a safe and effective therapeutic remedy for HN has aroused the interest of many researchers. FGF21 has emerged as an interesting hormone that starts increasing in early-stage chronic kidney disease [13]. Thus, in this study, we detected the expression

level of FGF21 in HN patients. We found that the content of FGF21 in the PBMCs of HN patients increased significantly. However, metabolic disorder often existing in HN disease may be the reason for the increase of FGF21 level in PBMCs. For this reason, we also detected the level of FGF21 in kidney of HN mice, and the results showed that the expression of FGF21 in kidney of HN mice was higher than that of normal control group, which suggested that FGF21 might participate in the process of HN. Therefore to determine the effect of FGF21 in HN, low and high doses of FGF21 were used.

First of all, we found that FGF21 significantly improved renal dysfunction associated with hyperuricemia. This was manifested through the restoration of the levels of BUN, Scr, CysC, and β2-MG, and an observed repairment of kidney injury evident from the H&E staining. Hence, the elevation of FGF21 may be considered as urvival response against major stress. We then observe the effect of FGF21 on renal injury complicated by hyperuricemia. Studies have shown that abnormal uric acid metabolism promotes the development of chronic inflammation [27, 28]. Therefore markers of inflammation were determined in the kidney of the mice. In the case of tissue injury, monocytes in blood are recruited to the injured site, and then differentiate into macrophages according to the exposed microenvironment signals. Macrophage infiltration in kidney is a common feature of human kidney diseases and is closely related to the severity of inflammation [29]. The activation of macrophages leads to the secretion of pro-inflammatory cytokines such as TNF-α, IL-1β, and IL-6, causing damage to the body [30]. Through the use of F4/80 immunohistochemistry in this study, we found that FGF21 significantly reduced the infiltration of macrophages in the kidney. Again the expressions of IL-1β, TNF-α, and IL-6 were also significantly abated tied to an upsurge in the expression of anti-inflammatory factor IL-10 after FGF21 treatment. In addition, the deposition of local urate crystals can mediate inflammatory reaction through the activation of inflammatory corpuscle NLRP3 [31]. However, we also found that FGF21 intervention significantly inhibited the expression of NLRP3. These data are suggestive of the anti-inflammatory effect of FGF21 in kidney injury associated with hyperuricemia.

Fibrosis is also a frequent manifestation of HN due to the excessive deposition of extracellular matrix (ECM) in the kidney [32]. The ECM is mainly composed of collagen, fibronectin, and other proteins [33]. In this study, Masson staining revealed a significant increase in collagen fibres in the model group. This was buttressed by western blotting results also recording a significant increase in α-SMA and Col1 in the kidney. After FGF21 treatment, however, these fibrotic markers were significantly decreased. TGF-β signalling pathway is the main pathway that leads to fibrosis in most chronic renal diseases [34]. In this study, FGF21 proved its anti-fibrotic effect by significantly inhibiting TGF-β.

Next, we explored the possible anti-inflammatory and anti-fibrotic mechanisms employed by FGF21. Studies suggest that oxidative stress plays an important role in the process of inflammation. ROS produced by oxidative stress can promote the aggregation and activation of NLRP3 inflammasome promoting the release of IL-1β, IL-18, and other inflammatory factors which in turn induce the production of ROS [5, 35]. This results in a vicious cycle as ROS further activates TGF-β to aggravate the fibrotic process [36]. In this study, however, FGF21 significantly inhibited ROS levels in hyperuricemic nephropathy mice and MSU and LPS treated GMCs. FGF21, again, significantly increased antioxidant

enzymes culminating in the observed improvement in oxidative stress. Nrf2 plays a key role in oxidative stress by binding to Keap1 to inhibit the expression of antioxidant enzymes. However, when stimulated by oxidative signals, Nrf2 uncouples with Keap1 and bind to AREs to up-regulate the expression of antioxidant enzymes [26]. Akt plays an important role in cell survival and apoptosis as it activates a variety of enzymes and transcription factors to regulate cell function [37]. Some studies have shown that Akt signalling pathway induced by cyclic stretching of mouse type 2 alveolar epithelial cells is inhibited in the presence of ROS inhibitor dibasic iodobenzene [38]. Other studies have also shown that FGF21 can promote the expression of Akt [39]. Therefore, it was speculated that FGF21 may regulate Nrf2 through Akt. In both i*n vivo* and *in vitro* experiments, FGF21 significantly increased the phosphorylation level of Akt and the nuclear accumulation of Nrf2. However, when the Akt inhibitor GSK690693 was added to GMCs, the expression of Nrf2 was significantly decreased, which indicated that FGF21 increased the expression of Nrf2 through Akt leading to the inhibition of glomerulonephritis and renal fibrosis (Fig. 7). Finally, although FGF21 could not reduce the level of uric acid (data not shown), its significant improvement of renal injury is encouraging warranting further research focusing on the combination of FGF21 with other uric acid-lowering drugs.

In conclusion, this study has found for the first time that FGF21 can significantly improve renal injury in hyperuricemia. These beneficial effects are achieved by activating Akt/Nrf2 signal pathway to improve oxidative stress.

Declarations

Funding This work was supported by the National Key R&D Program of China [grant numbers 2017YFD0501102, 2017YFD0501004, 2016YFD0501003]; Science and Technology Department of Heilongjiang Province [grant number GX18B018] and Education Department of Heilongjiang Province [grant number TSTAU-R2018017].

Conflict of interest statement

The authors have no relevant financial or non-financial interests to disclose.

Availability of data and material The datasets generated during and/or analysed during the current study are available from the corresponding author on reasonable request.

Code availability Not applicable

Author contributions All authors contributed to the study conception and design. Guiping Ren and Deshan Li designed the study. Xinghao Jiang, Shijie Liu and Dan Wang performed the research. Yeboah Kwaku Opoku wrote the paper. Yimeng Zou and Kai Kang analyzed the data. All authors read and approved the final manuscript.

Ethics approval

All study participants signed written consent forms to be enrolled in the study with the confidentiality of their data assured. This study was approved by the Ethics Committee of the Endocrinology Department of Harbin First Hospital. All animal studies were conducted in accordance with the guidelines formulated by the Animal Protection and Utilization Committee of Northeast Agricultural University.

Consent to participate Not applicable

Consent for publication Not applicable

References

[1] Ramirez-Sandoval, J. C., & Madero, M. (2018). Treatment of Hyperuricemia in Chronic Kidney Disease. Contrib Nephrol, 192, 135-146. doi:10.1159/000484288

[2] Lima, W. G., Martins-Santos, M. E., & Chaves, V. E. (2015). Uric acid as a modulator of glucose and lipid metabolism. Biochimie, 116, 17-23. doi:10.1016/j.biochi.2015.06.025

[3] Battelli, M. G., Polito, L., Bortolotti, M., & Bolognesi, A. (2016). Xanthine Oxidoreductase in Drug Metabolism: Beyond a Role as a Detoxifying Enzyme. Current Medicinal Chemistry, 23(35), 4027-4036. doi:10.2174/0929867323666160725091915

[4] Isaka, Y., Takabatake, Y., Takahashi, A., Saitoh, T., & Yoshimori, T. (2016). Hyperuricemia-induced inflammasome and kidney diseases. Nephrol Dial Transplant, 31(6), 890-896. doi:10.1093/ndt/gfv024

[5] Liu, X., Zhao, X., Duan, X., Wang, X., Wang, T., Feng, S., . . . Li, G. (2021). Knockout of NGAL aggravates tubulointerstitial injury in a mouse model of diabetic nephropathy by enhancing oxidative stress and fibrosis. Exp Ther Med, 21(4), 321. doi:10.3892/etm.2021.9752

[6] Li, C., Hsieh, M. C., & Chang, S. J. (2013). Metabolic syndrome, diabetes, and hyperuricemia. Curr Opin Rheumatol, 25(2), 210-216. doi:10.1097/BOR.0b013e32835d951e

[7] Becker, M. A., Schumacher, H. R., Jr., Wortmann, R. L., MacDonald, P. A., Eustace, D., Palo, W. A., . . . Joseph-Ridge, N. (2005). Febuxostat compared with allopurinol in patients with hyperuricemia and gout. N Engl J Med, 353(23), 2450-2461. doi:10.1056/NEJMoa050373

[8] Vargas-Santos, A. B., & Neogi, T. (2017). Management of Gout and Hyperuricemia in CKD. Am J Kidney Dis, 70(3), 422-439. doi:10.1053/j.ajkd.2017.01.055

[9] Jordan, A., & Gresser, U. (2018). Side Effects and Interactions of the Xanthine Oxidase Inhibitor Febuxostat. Pharmaceuticals (Basel), 11(2). doi:10.3390/ph11020051

[10] Zeng, X. X., Tang, Y., Hu, K., Zhou, X., Wang, J., Zhu, L., . . . Xu, J. (2018). Efficacy of febuxostat in hyperuricemic patients with mild-to-moderate chronic kidney disease: a meta-analysis of randomized

clinical trials: A PRISMA-compliant article. Medicine (Baltimore), 97(13), e0161. doi:10.1097/md.0000000000010161

[11] Nishimura, T., Nakatake, Y., Konishi, M., & Itoh, N. (2000). Identification of a novel FGF, FGF-21, preferentially expressed in the liver. Biochim Biophys Acta, 1492(1), 203-206. doi:10.1016/s0167-4781(00)00067-1

[12] BonDurant, L. D., & Potthoff, M. J. (2018). Fibroblast Growth Factor 21: A Versatile Regulator of Metabolic Homeostasis. Annu Rev Nutr, 38, 173-196. doi:10.1146/annurev-nutr-071816-064800

[13] Salgado, J. V., Goes, M. A., & Salgado Filho, N. (2021). FGF21 and Chronic Kidney Disease. Metabolism-Clinical And Experimental, 118, 154738. doi:10.1016/j.metabol.2021.154738

[14] Fisher, F. M., & Maratos-Flier, E. (2016). Understanding the Physiology of FGF21. Annu Rev Physiol, 78, 223-241. doi:10.1146/annurev-physiol-021115-105339

[15] Dolegowska, K., Marchelek-Mysliwiec, M., Nowosiad-Magda, M., Slawinski, M., & Dolegowska, B. (2019). FGF19 subfamily members: FGF19 and FGF21. Journal Of Physiology And Biochemistry, 75(2), 229-240. doi:10.1007/s13105-019-00675-7

[16] Kim, J. H., Lee, G. Y., Maeng, H. J., Kim, H., Bae, J. H., Kim, K. M., & Lim, S. (2021). Effects of Glucagon-Like Peptide-1 Analogue and Fibroblast Growth Factor 21 Combination on the Atherosclerosis-Related Process in a Type 2 Diabetes Mouse Model. Endocrinol Metab (Seoul), 36(1), 157-170. doi:10.3803/EnM.2020.781

[17] Adams, A. C., Halstead, C. A., Hansen, B. C., Irizarry, A. R., Martin, J. A., Myers, S. R., . . . Kharitonenkov, A. (2013). LY2405319, an Engineered FGF21 Variant, Improves the Metabolic Status of Diabetic Monkeys. Plos One, 8(6), e65763. doi:10.1371/journal.pone.0065763

[18] Jiang, X., Liu, S., Wang, Y., Zhang, R., Opoku, Y. K., Xie, Y., . . . Ren, G. (2020). Fibroblast growth factor 21: a novel long-acting hypoglycemic drug for canine diabetes. Naunyn Schmiedebergs Arch Pharmacol. doi:10.1007/s00210-020-02023-9

[19] Jimenez, V., Jambrina, C., Casana, E., Sacristan, V., Muñoz, S., Darriba, S., . . . Bosch, F. (2018). FGF21 gene therapy as treatment for obesity and insulin resistance. EMBO Mol Med, 10(8). doi:10.15252/emmm.201708791

[20] Yu, D., Ye, X., Che, R., Wu, Q., Qi, J., Song, L., . . . Li, D. (2017). FGF21 exerts comparable pharmacological efficacy with Adalimumab in ameliorating collagen-induced rheumatoid arthritis by regulating systematic inflammatory response. Biomed Pharmacother, 89, 751-760. doi:10.1016/j.biopha.2017.02.059

[21] Chen, S., Chen, D., Yang, H., Wang, X., Wang, J., & Xu, C. (2020). Uric acid induced hepatocytes lipid accumulation through regulation of miR-149-5p/FGF21 axis. BMC Gastroenterol, 20(1), 39.

doi:10.1186/s12876-020-01189-z

[22] Pan, J., Shi, M., Li, L., Liu, J., Guo, F., Feng, Y., . . . Fu, P. (2019). Pterostilbene, a bioactive component of blueberries, alleviates renal fibrosis in a severe mouse model of hyperuricemic nephropathy. Biomed Pharmacother, 109, 1802-1808. doi:10.1016/j.biopha.2018.11.022

[23] Zhang, S., Yu, D., Wang, M., Huang, T., Wu, H., Zhang, Y., . . . Li, D. (2018). FGF21 attenuates pulmonary fibrogenesis through ameliorating oxidative stress in vivo and in vitro. Biomed Pharmacother, 103, 1516-1525. doi:10.1016/j.biopha.2018.03.100

[24] Wang, N., Li, J. Y., Li, S., Guo, X. C., Wu, T., Wang, W. F., & Li, D. S. (2018). Fibroblast growth factor 21 regulates foam cells formation and inflammatory response in Ox-LDL-induced THP-1 macrophages. Biomed Pharmacother, 108, 1825-1834. doi:10.1016/j.biopha.2018.09.143

[25] Nikolic-Paterson, D. J., & Atkins, R. C. (2001). The role of macrophages in glomerulonephritis. Nephrol Dial Transplant, 16 Suppl 5, 3-7. doi:10.1093/ndt/16.suppl_5.3

[26] Bellezza, I., Giambanco, I., Minelli, A., & Donato, R. (2018). Nrf2-Keap1 signaling in oxidative and reductive stress. Biochim Biophys Acta Mol Cell Res, 1865(5), 721-733. doi:10.1016/j.bbamcr.2018.02.010

[27] Karbowska, A., Boratynska, M., Kusztal, M., & Klinger, M. (2009). Hyperuricemia is a mediator of endothelial dysfunction and inflammation in renal allograft recipients. Transplant Proc, 41(8), 3052-3055. doi:10.1016/j.transproceed.2009.07.080

[28] Kimura, Y., Yanagida, T., Onda, A., Tsukui, D., Hosoyamada, M., & Kono, H. (2020). Soluble Uric Acid Promotes Atherosclerosis via AMPK (AMP-Activated Protein Kinase)-Mediated Inflammation. Arterioscler Thromb Vasc Biol, 40(3), 570-582. doi:10.1161/atvbaha.119.313224

[29] Watanabe, S., Alexander, M., Misharin, A. V., & Budinger, G. R. S. (2019). The role of macrophages in the resolution of inflammation. J Clin Invest, 129(7), 2619-2628. doi:10.1172/jci124615

[30] Hotchkiss, K. M., Reddy, G. B., Hyzy, S. L., Schwartz, Z., Boyan, B. D., & Olivares-Navarrete, R. (2016). Titanium surface characteristics, including topography and wettability, alter macrophage activation. Acta Biomater, 31, 425-434. doi:10.1016/j.actbio.2015.12.003

[31] Youm, Y. H., Nguyen, K. Y., Grant, R. W., Goldberg, E. L., Bodogai, M., Kim, D., . . . Dixit, V. D. (2015). The ketone metabolite β-hydroxybutyrate blocks NLRP3 inflammasome-mediated inflammatory disease. Nat Med, 21(3), 263-269. doi:10.1038/nm.3804

[32] Johnson, R. J., Nakagawa, T., Jalal, D., Sánchez-Lozada, L. G., Kang, D. H., & Ritz, E. (2013). Uric acid and chronic kidney disease: which is chasing which? Nephrol Dial Transplant, 28(9), 2221-2228. doi:10.1093/ndt/gft029

[33] Ricard-Blum, S., Baffet, G., & Théret, N. (2018). Molecular and tissue alterations of collagens in fibrosis. Matrix Biol, 68-69, 122-149. doi:10.1016/j.matbio.2018.02.004

[34] Meng, X. M., Nikolic-Paterson, D. J., & Lan, H. Y. (2016). TGF-β: the master regulator of fibrosis. Nat Rev Nephrol, 12(6), 325-338. doi:10.1038/nrneph.2016.48

[35] Han, Y., Xu, X., Tang, C., Gao, P., Chen, X., Xiong, X., . . . Sun, L. (2018). Reactive oxygen species promote tubular injury in diabetic nephropathy: The role of the mitochondrial ros-txnip-nlrp3 biological axis. Redox Biol, 16, 32-46. doi:10.1016/j.redox.2018.02.013

[36] Liu, R. M., & Gaston Pravia, K. A. (2010). Oxidative stress and glutathione in TGF-beta-mediated fibrogenesis. Free Radic Biol Med, 48(1), 1-15. doi:10.1016/j.freeradbiomed.2009.09.026

[37] Abeyrathna, P., & Su, Y. (2015). The critical role of Akt in cardiovascular function. Vascul Pharmacol, 74, 38-48. doi:10.1016/j.vph.2015.05.008

[38] Lee, Y. J., Jeong, H. Y., Kim, Y. B., Lee, Y. J., Won, S. Y., Shim, J. H., . . . Lee, S. H. (2012). Reactive oxygen species and PI3K/Akt signaling play key roles in the induction of Nrf2-driven heme oxygenase-1 expression in sulforaphane-treated human mesothelioma MSTO-211H cells. Food Chem Toxicol, 50(2), 116-123. doi:10.1016/j.fct.2011.10.035

[39] Yu, Y., Bai, F., Liu, Y., Yang, Y., Yuan, Q., Zou, D., . . . Li, D. (2015). Fibroblast growth factor (FGF21) protects mouse liver against D-galactose-induced oxidative stress and apoptosis via activating Nrf2 and PI3K/Akt pathways. Mol Cell Biochem, 403(1-2), 287-299. doi:10.1007/s11010-015-2358-6

Figures

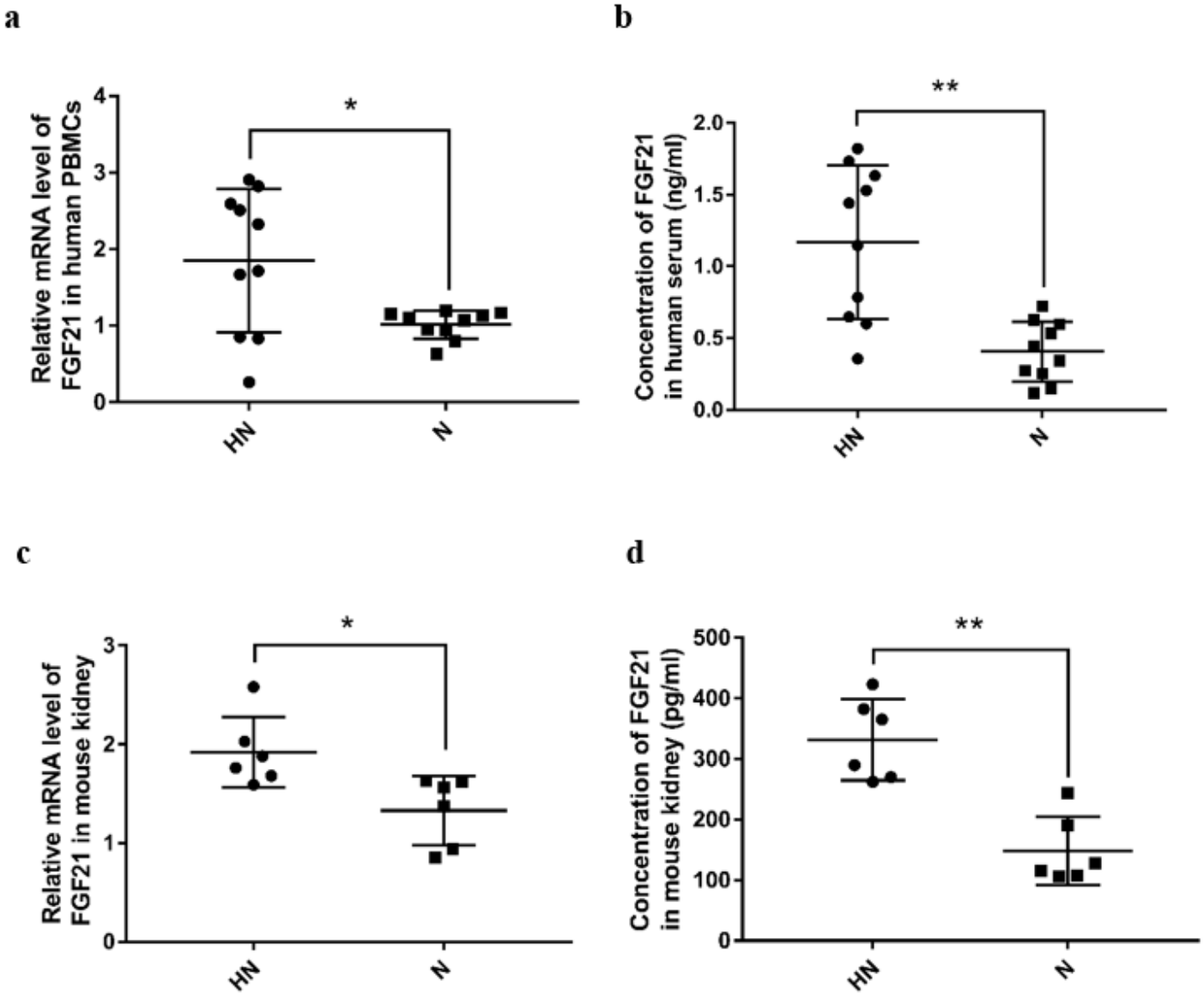

Figure 1

Enhanced levels of FGF21 in patients and mice with HN. RNA and protein were extracted from human PBMCs or mouse kidney for the detection of FGF21 by qPCR and Elisa. HN: hyperuricemic nephropathy, N: normal control. (a) qPCR analysis of FGF21 mRNA level in human PBMCs, n=10. (b) Elisa analysis of FGF21 protein level in human serum, n=10. (c) qPCR analysis of FGF21 mRNA level in mouse kidney, n=6. (d) Elisa analysis of FGF21 protein level in mouse kidney, n=6. The mean ± SD is plotted as indicated by the error bars. Significant as compared to N, *P<0.05, **P<0.01.

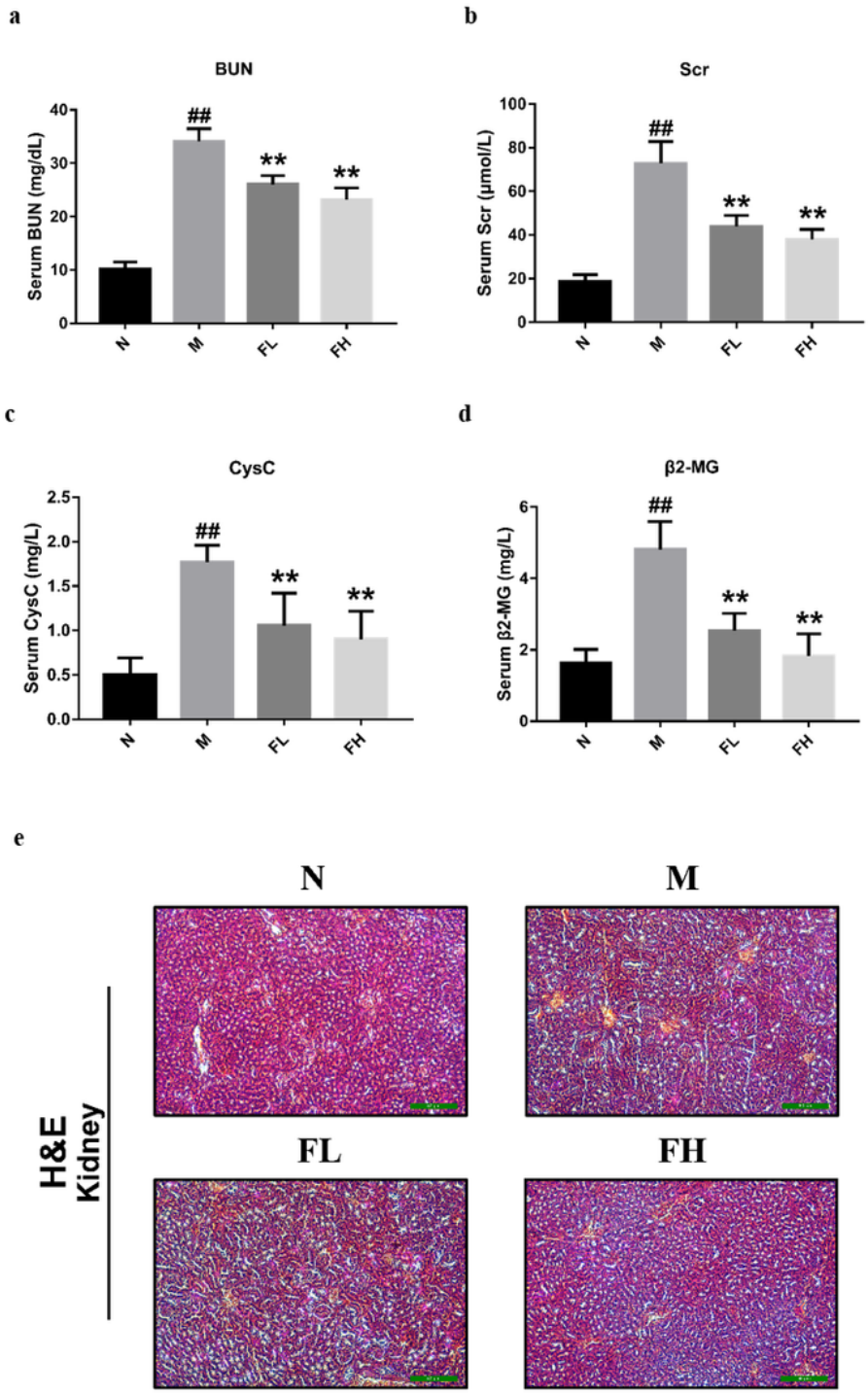

Figure 2

FGF21 ameliorates renal function damage in HN mice. N: normal control group; M: model control group; FL: FGF21 low dose group; FH: FGF21 high dose group. (a)-(d) Renal function indexes of mice. The mean ± SD is plotted as indicated by the error bars, n=6. Significant as compared to N, ##P<0.01; Significant as compared to M, *P<0.05, **P<0.01. (e) H&E staining of kidney in each group of mice.

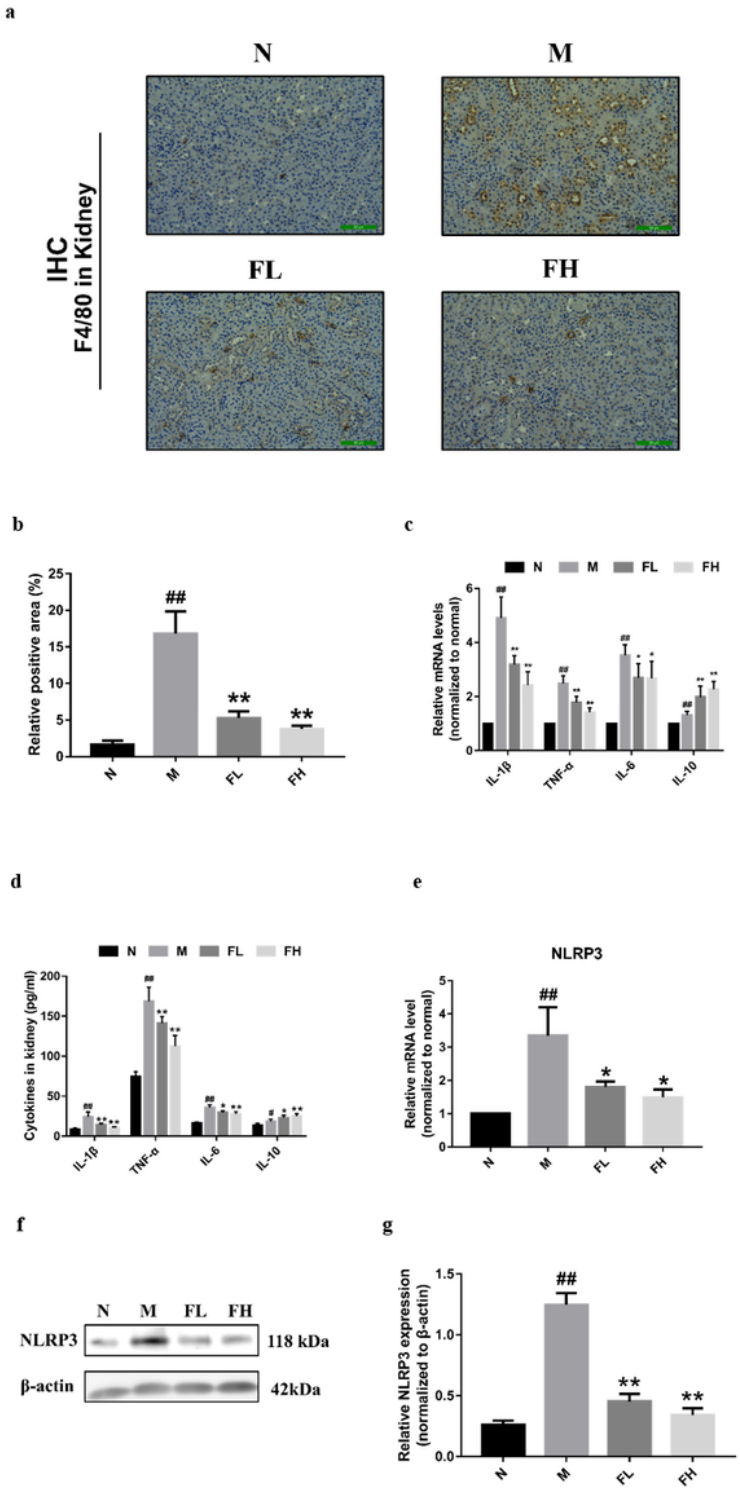

Figure 3

FGF21 reduced renal inflammation in HN mice. N: normal control group; M: model control group; FL: FGF21 low dose group; FH: FGF21 high dose group. (a) Immunohistochemical analysis of the infiltration of renal macrophages in HN mice. (b) Quantitative analysis of immunohistochemical positive rate, n=3. (c) The relative content of IL-1β, TNF-α, IL-6 and IL-10 mRNA levels in renal, n=6. (d) Elisa analysis of IL-1β, TNF-α, IL-6 and IL-10 protein levels in renal, n=6. (e) The relative content of NLRP3 mRNA level in

kidney, n=3 (f) Western blotting analysis of NLRP3 in kidney and quantifications (g), n=3. The mean ± SD is plotted as indicated by the error bars. Significant as compared to N, #P<0.05, ##P<0.01; Significant as compared to M, *P<0.05, **P<0.01.

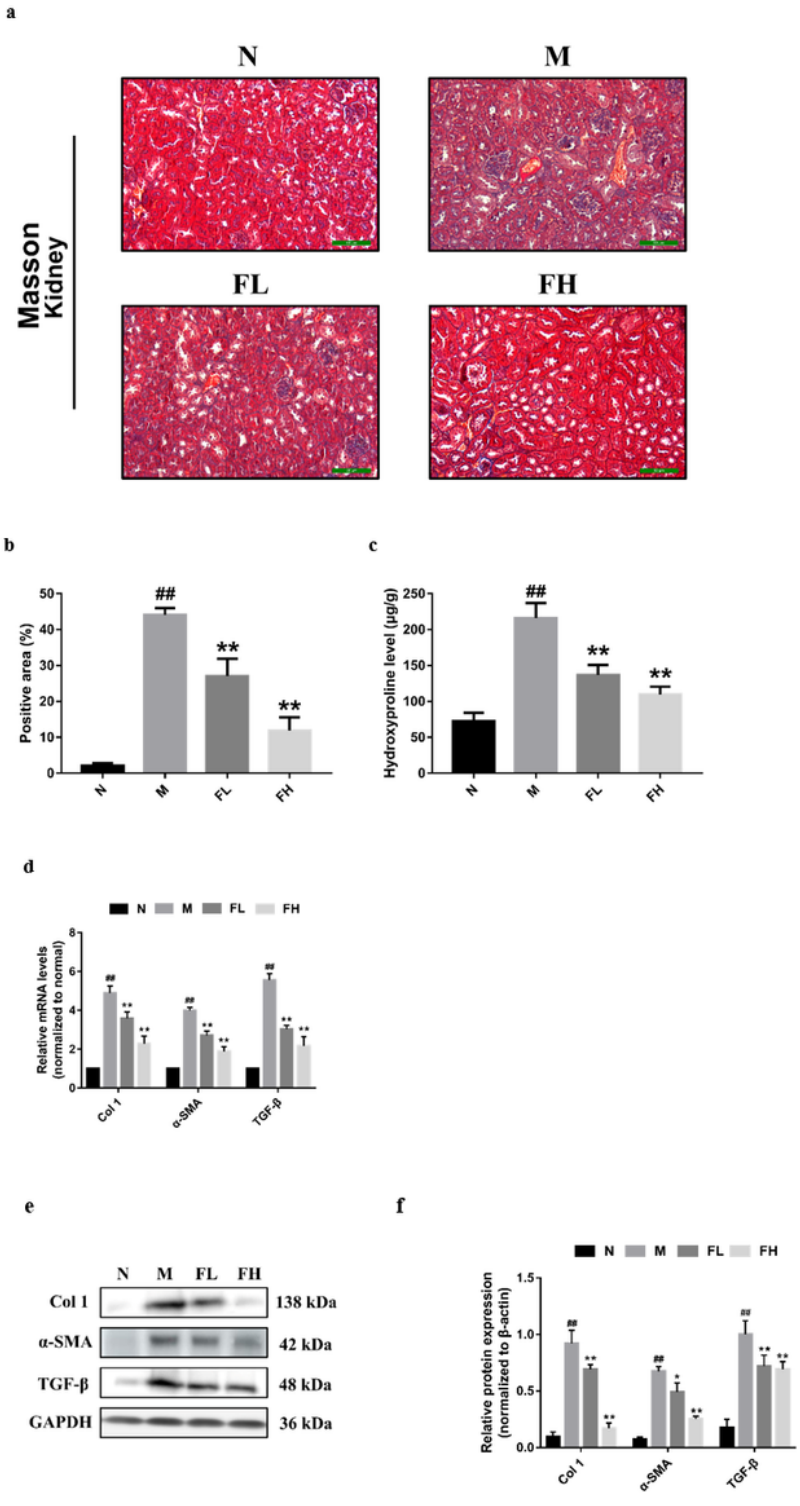

Figure 4

FGF21 improves renal fibrosis in HN mice. N: normal control group; M: model control group; FL: FGF21 low dose group; FH: FGF21 high dose group. (a) Masson staining of kidney in each group of mice. (b)

Relative positive areas of Masson staining, n=3 (c) Content of hydroxyproline in kidney in each group of mice, n=6. (d) The relative content of Col 1, α-SMA and TGF-β mRNA levels in kidney, n=3. (e) Western blotting analysis of Col 1, α-SMA and TGF-β in kidney and quantifications (f), n=3. The mean ± SD is plotted as indicated by the error bars, n=3. Significant as compared to N, #P<0.05, ##P<0.01; Significant as compared to M, *P<0.05, **P<0.01.

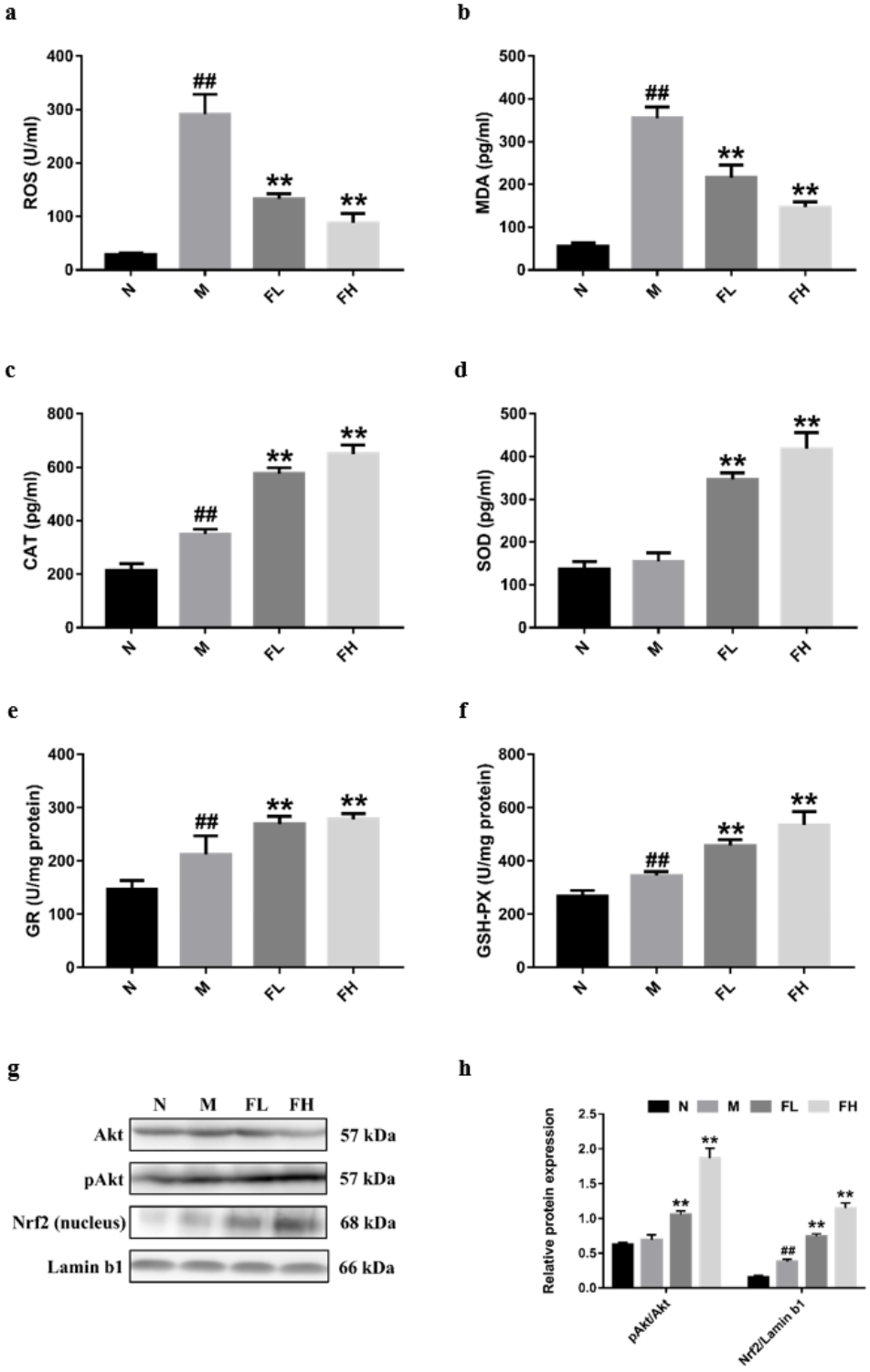

Figure 5

FGF21 ameliorates oxidative stress in HN mice. N: normal control group; M: model control group; FL: FGF21 low dose group; FH: FGF21 high dose group. (a)-(f) Elisa analysis of ROS, MDA, CAT, SOD, GR and GSH-PX in kidney, n=6. (g) Western blotting analysis of Akt, pAkt and Nrf2 in kidney and quantifications (h), n=3. The mean ± SD is plotted as indicated by the error bars, n=3. Significant as compared to N, ##P<0.01; Significant as compared to M, **P<0.01.

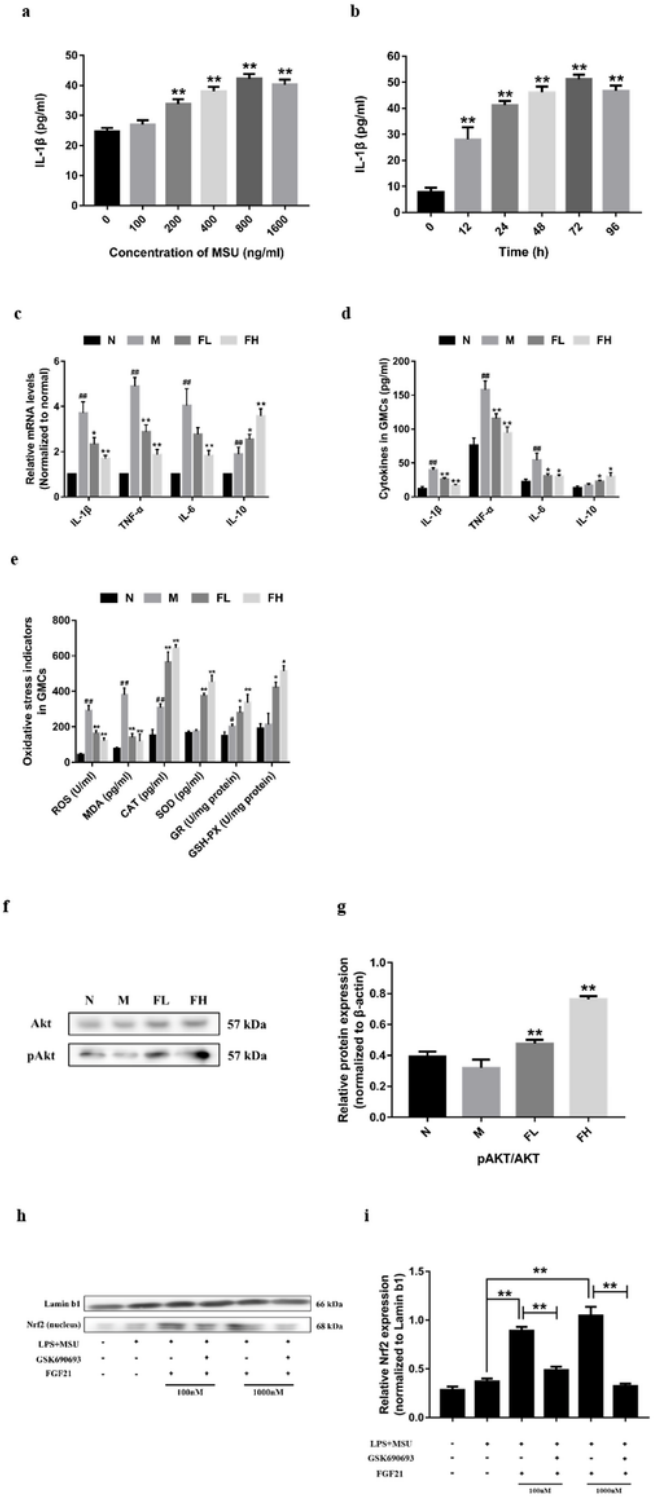

Figure 6

FGF21 ameliorates oxidative stress through Akt/Nrf2 signal pathway in GMCs. N: normal control group; M: model control group; FL: FGF21 low dose group; FH: FGF21 high dose group. Cells were treated with LPS (500 ng/ml), MSU (800 ng/ml) and different concentrations of FGF21 (with or without GSK690693) for 72 hours. (a) Elisa analysis of IL-1β content in GMCs at different MSU concentrations, n=3. Significant as compared to 0, **P<0.01. (b) Elisa analysis of IL-1β content in GMCs with different action time, n=3. Significant as compared to 0, **P<0.01. (c) qPCR analysis of IL-1β, TNF-α, IL-6, and IL-10 levels in GMCs, n=3. (d) Elisa analysis of IL-1β, TNF-α, IL-6, and IL-10 levels in GMCs, n=3. (e) Elisa analysis of ROS, MDA, CAT, SOD, GR, and GSH-PX levels in GMCs, n=3. (f) Western blotting analysis of AKT and pAKT levels in GMCs and quantifications (g), n=3. (h) Western blotting analysis of nuclear accumulation of Nrf2 level in GMCs and quantifications (i), n=3. The mean ± SD is plotted as indicated by the error bars, n=3. Significant as compared to N, #P<0.05, ##P<0.01; Significant as compared to M, *P<0.05, **P<0.01.

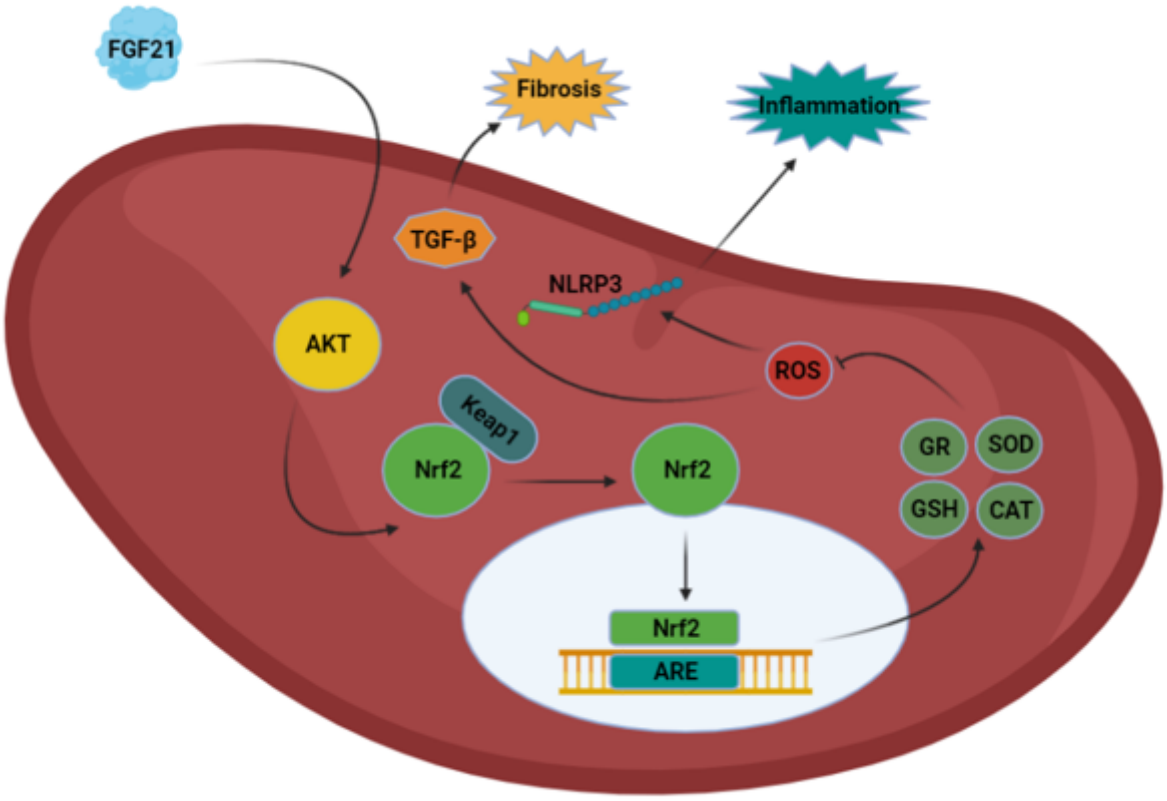

Figure 7

Schematic molecular mechanism underlying the improvement of HN by FGF21. FGF21 activates Akt to promote the uncoupling of Nrf2 and Keap1 making Nrf2 to combine with AREs to promote the release of antioxidant enzymes. Antioxidant enzymes inhibit the expression of ROS, and then inhibit NLRP3-mediated inflammation and the expression of TGF- β to improve fibrosis.